Boundary-Layer Meteorology (2005) 114: 413–437

NUMERICAL SIMULATIONS OF KATABATIC JUMPS IN COATS LAND, ANTARCTICA

YE YU[1,*], XIAOMING CAI[1], JOHN C. KING[2] and IAN A. RENFREW[2]
[1]*School of Geography, Earth and Environmental Sciences, The University of Birmingham, Edgbaston, Birmingham B15 2TT, U.K.;* [2]*Physical Sciences Division, British Antarctic Survey, Natural Environment Research Council, High Cross, Madingley Road, Cambridge, CB3 0ET, U.K.*

(Received in final form 26 April 2004)

Abstract. A non-hydrostatic numerical model, the Regional Atmospheric Modeling System (RAMS), has been used to investigate the development of katabatic jumps in Coats Land, Antarctica. In the control run with a 5 m s^{-1} downslope directed initial wind, a katabatic jump develops near the foot of the idealized slope. The jump is manifested as a rapid deceleration of the downslope flow and a change from supercritical to subcritical flow, in a hydraulic sense, i.e., the Froude number (*Fr*) of the flow changes from $Fr > 1$ to $Fr < 1$. Results from sensitivity experiments show that an increase in the upstream flow rate strengthens the jump, while an increase in the downstream inversion-layer depth results in a retreat of the jump. Hydraulic theory and Bernoulli's theorem have been used to explain the surface pressure change across the jump. It is found that hydraulic theory always underestimates the surface pressure change, while Bernoulli's theorem provides a satisfactory estimation. An analysis of the downslope momentum balance for the katabatic jump indicates that the important forces are those related to the pressure gradient, advection and, to a lesser extent, the turbulent momentum divergence. The development of katabatic jumps can be divided into two phases. In phase I, the pressure gradient force is nearly balanced by advection, while in phase II, the pressure gradient force is counterbalanced by turbulent momentum divergence. The upslope pressure gradient force associated with a pool of cold air over the ice shelf facilitates the formation of the katabatic jump.

Keywords: Antarctica, Bernoulli's theorem, Hydraulic theory, Katabatic jump, Momentum balance, Pressure change.

1. Introduction

The near-surface airflow over the Antarctic continent is strongly influenced by strong and persistent katabatic winds resulting from the radiative cooling of the sloping surface of the continental ice sheets (Parish, 1988). It is recognized that this low-level drainage flow is an important component of the large-scale atmospheric circulation over the Antarctic continent (Parish, 1992; Parish et al., 1994). Regions of strong katabatic winds also play an important role in the energy budget of the South Polar regions by main-

* E-mail: yyuds@yahoo.co.uk

taining coastal open water areas (polynyas) (Bromwich and Kurtz, 1984; Adolphs and Wendler, 1995). Besides the violence and persistence of these katabatic winds, a sudden breakdown or cessation, known as a 'katabatic jump' or 'Loewe's Phenomenon', has been reported in some coastal regions of the Antarctica (Madigan, 1929 reported by Ball, 1956; Lied, 1964; Pettré and André, 1991, hereafter PA91). This sudden cessation of katabatic winds, through katabatic jumps, limits the extent of the katabatic flow from the Antarctic and has potential effects on the general circulation and thus the climate system. In the past 20 years a number of studies have been devoted to the large-scale dynamics and patterns of katabatic flows over the Antarctic (e.g., Parish and Bromwich, 1987; Bromwich, 1989), but very few to the small-scale dynamics involved in katabatic jumps.

A katabatic jump, named by analogy to the hydraulic jumps found in open channel flows, is characterized by a narrow region of rapid transition from strong katabatic flow to near-calm conditions. In terms of hydraulic theory, this corresponds to a change from supercritical (Froude number $Fr > 1$) to subcritical ($Fr < 1$) flow conditions. Katabatic jumps have been frequently quoted in the reports of Antarctic explorers, but *in situ* observations are relatively rare, e.g., Lied (1964) and PA91. This is due to the difficulty of collecting data with existing instrumentation under the severe weather conditions that accompany the katabatic jumps and their transient nature. Nevertheless, these limited observations have revealed some common characteristics of katabatic jumps, including a wall of drifting snow and intense turbulence in the narrow jump region. A detailed description of these characteristics can be found in King and Turner (1997).

Recently there have been some attempts at interpreting the occurrence of katabatic jumps using numerical models. Gallée and Schayes (1992), using a two-dimensional hydrostatic model, studied the spatial evolution of katabatic winds over two different constant slopes. In one of their simulations (with 5% slope) a sudden transition from a strong katabatic wind to a weak upslope flow was produced about 10–20 km inland from the foot of the slope. This transition was attributed to a discontinuity of the potential temperature field near the foot of the slope. Although the detailed structure within the katabatic jump could not be derived from their hydrostatic model, Gallée and Schayes' results suggested that the rapid adjustment from a katabatic flow to a calm condition might occur frequently in coastal regions. Recently Gallée et al. (1996) and Gallée and Pettré (1998) performed a more comprehensive simulation of the evolution of summer katabatic wind events in Adélie Land, Antarctica, using observed soundings as initial and boundary conditions. Their results revealed the importance of the unstable layer formed above the cold katabatic layer and the piling up of cold air near the coast under strong, downslope directed large-scale winds for the sharp spatial transition from downslope katabatic flow to upslope winds. Although this work revealed possible hydrostatic processes that were responsible for the occurrence of katabatic flow jumps, the strong vertical accelerations, indicated by the observed wall of blowing snow and strong turbulence, are not reproducible in their simulations due to the *hydrostatic* formulation of the model.

While previous studies have focused upon climatologically strong katabatic wind areas, for example, the Adélie Land coast (Gallée et al., 1996; Gallée and Pettré, 1998), recent studies in a moderate katabatic wind area – Coats Land, Antarctica (Figure 1) – have revealed several interesting features concerning the flow behaviour over the Brunt Ice Shelf. For example, King (1993), based on wind observations from two ice shelf sites, showed that the flow over the ice shelf cannot be explained as the result of a simple

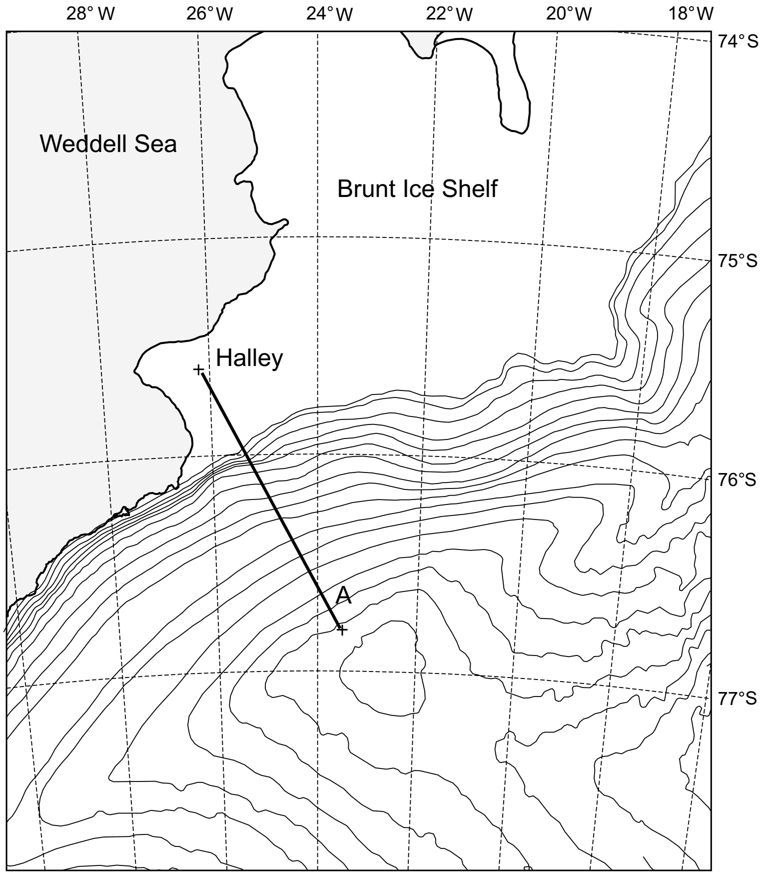

Figure 1. A map of the Coats Land region of Antarctica, showing some of the locations mentioned in the text. The contour interval is 100 m. The line 'A' marks the route of Peel's (1976) traverse.

inertial adjustment of the downslope flow from the adjoining continental slope and suggested that a katabatic jump may exist. A more recent climatological analysis of 5 years' automatic weather station (AWS) data confirmed that there were two different surface-flow regimes in this area, one over the continent and one over the adjoining ice shelf (Renfrew and Anderson, 2002).

Our study investigates katabatic jumps in the Coats Land area using a non-hydrostatic regional atmospheric model. Clearly, the observed sharp transitions of katabatic flow are a non-hydrostatic phenomenon, and thus simulations using non-hydrostatic models should give more realistic results. The numerical model and its configuration are described in Section 2, while Section 3 presents the model results and assesses the response of the katabatic flow to different upstream and downstream flow conditions. A discussion of the occurrence of katabatic jumps is also included in this section; the summary and conclusions are presented in Section 4.

2. The Numerical Model

The Regional Atmospheric Modeling System (RAMS) used for the simulation is version 4.3.0. A general description of the model and its parameterizations is given in Pielke et al. (1992) and Cotton et al. (2003) while a summary of the characteristics used in this paper can be found in Table I.

TABLE I
RAMS characteristics used in this paper.

	RAMS
Grid	Arakawa-C
Vertical coordinate	Terrain-following σ_z
Horizontal coordinate	Rotated polar-stereographic transformation
Equations of motion	Non-hydrostatic, compressible
Surface layer	Louis (1979)
Turbulence closure	*Horizontal*: Smagorinsky (1963) deformation, $c_s = 0.3$ *Vertical*: Mellor–Yamada level 2.5 (Mellor and Yamada, 1982)
Radiation	Longwave radiation only (Mahrer and Pielke, 1979)
Microphysics	Vapour phase only without condensation
Lower boundary	Soil/vegetation/snow parameterization (LEAF-2, Walko et al., 2000), adapted for firn (compacted snow) (Renfrew, 2004)
Upper boundary	Rigid lid, damping with Rayleigh friction

For the present studies, a 24-hr 'pre-integration' was performed over a domain of $100 \times 10 \times 40$ grid points (in x-, y- and z-directions, respectively) with constant grid spacing of 3.5 km in both the x- and y-directions and a stretched grid structure in the z-direction. This specification of model domain is based on the assumption of a two-dimensional (2D) flow for the case investigated. This is reasonable as observations indicate that the topography of Coats Land, Antarctica, is approximately two-dimensional (see Figure 1). The purpose of the 24-hr pre-integration is to set up a basic model flow response, which can then be modified for the sensitivity experiments. The 24-hr pre-integration is initialized using horizontally homogeneous temperature and humidity fields taken from a sounding from the Halley research station (75.6° S, 26.2° W) made on 7 May 1999 at 1100 UTC. An initial background wind (u_0) of 5 m s^{-1} in the downslope direction is set throughout the domain. Simulations with the same strength of downslope wind but different wind directions lead to similar results (Yu, 2004). Mixed boundary conditions are applied for the 24-hr pre-integration: with radiative boundary conditions in the along-slope direction and periodic boundary conditions in the cross-slope direction. During the simulation the effects of solar radiation are not considered and the sea surface is assumed to be covered with thick sea ice, making the simulations representative of austral winter conditions. By the end of the 24-hr pre-integration a strongly stable surface layer is fully developed and a quasi-equilibrium condition with a katabatic jump prevails.

A 12-hr control run and a series of 12-hr sensitivity experiments are then executed on a smaller domain of $40 \times 10 \times 40$ grid points (in x-, y- and z-directions, respectively), using the analysis fields at the end of the 24-hr pre-integration, or its modifications, as initial and boundary conditions. The model adjusts to the modified field very quickly (in about 2 hrs) and reaches another quasi-equilibrium state within 12 hrs. Further integration beyond the 12-hr integration contributes little to the development of the modelled fields. For the control run and sensitivity experiments, three grids were nested to bring the horizontal grid spacing from 3500 m (Grid 1) to 700 m (Grid 2) and 175 m (Grid 3) (see Figure 2 for the domain size of nested grids). The control run was carried out using analysis fields at the end of the 24-hr pre-integration as initial and boundary conditions, i.e., the lateral boundaries were nudged toward the state at the end of the 24-hr pre-integration. Ideally, the control run and all the sensitivity experiments should be integrated over the whole domain rather than the smaller domain, but as no significant difference was detected when the control run was conducted over the whole domain, i.e., with $100 \times 10 \times 40$ grid points, the smaller domain is used for the control run, and all the sensitivity experiments in this paper, to focus on the area of the greatest interest, i.e., near the foot of the slope. For the sensitivity experiments, the initial and boundary conditions are modifications of the 24-hr

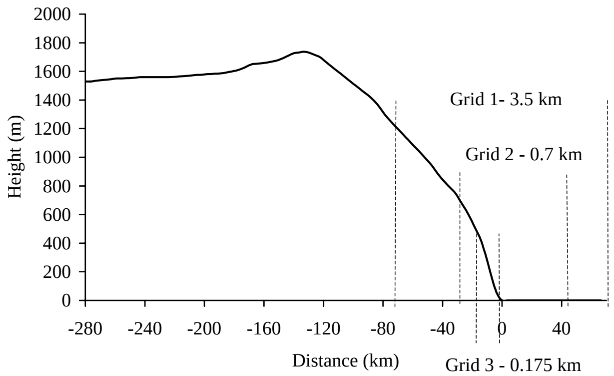

Figure 2. Terrain height used in pre-integration. The dashed lines indicate the model domain of the three grids used for the control run and sensitivity experiments.

pre-integration fields, as described in the next section. The control run and the sensitivity experiments were first run on Grids 1 and 2 for 6 hrs. After the 6-hr integration, Grid 3 was added. The grid spacing, number of grid points, and the time step of each of the three grids used in the control run and sensitivity experiments are shown in Table II. Vertically, all grids have the same 40 levels, with a vertical grid spacing starting at 5 m at the surface and stretching by a factor of 1.15 for each successive level above the surface (capped by a maximum value of 994 m), which results in a vertical height of the domain of about 8 km. A very good resolution of the boundary layer is achieved, as 15 of the 40 levels are located in the lowest 200 m of the atmosphere. The same vertical grid structure is used in the 24-hr pre-integration. The model output presented herein is at the end of the 12-hr integration following the 24-hr pre-integration.

The model topography used in the 24-hr pre-integration is displayed in Figure 2, which is the cross-section along line A in Figure 1. Dashed boxes mark the domain (in the x-direction) of the three grids used in the control and sensitivity experiments. The input data used in the simulations are listed in Table III.

TABLE II

Grid structure for control run and sensitivity experiments.

Grid	ΔX (m)	N_x	N_y	ΔT (s)
1	3500	40	10	4
2	700	102	12	1
3	175	102	18	0.3

TABLE III
List of the data used for all simulations.

Input data	
Initial surface temperature	King et al. (1998)
Initial air temperature	Sounding at Halley station
Topography	2D, from Peel (1976)
Roughness length and scalar roughness length	1×10^{-4} m

3. Results and Discussions

3.1. The control run

In the 24-hr pre-integration a well-defined katabatic flow develops over the slope and grows in strength over time reaching a quasi-steady state at the end of the 24-hr period. Figure 3 shows cross-sections of potential temperature (θ), downslope wind component (u) and turbulent kinetic energy (TKE) for Grid 1, where only the lowest 3000 m of elevation is shown. Note that the model uses terrain-following coordinates and the results shown in Figure 3 are for levels $k \leq 32$. Subject to the radiative cooling of the sloping surface, a strong inversion and conditions for maintaining a strong katabatic flow are established on the slope. The cross-section of the downslope wind component depicted in Figure 3b reveals a characteristic katabatic signature with a low-level maximum at about 80 m above the surface. The downslope wind field in Figure 3b exhibits a region of high-speed 'shooting flow' extending over most of the slope, terminating with a rapid decrease near the foot of the slope. This sudden decay of katabatic wind near the foot of a slope was also reported in other studies (e.g., PA91; Gallée and Pettré, 1998) and is related to a katabatic jump. Indeed, the flow changes rapidly from supercritical ($Fr_{\mathrm{m}} > 1$) to subcritical ($Fr_{\mathrm{m}} < 1$) near this region (see later in Figure 4c), which, in a hydraulic framework, can only occur through a discontinuity or a hydraulic jump.

An examination of the potential temperature field (Figure 3a) indicates that 'piling up of cold air' occurs near the foot of the slope and extends to the ice shelf. This 'piling up of cold air' has been found to be a possible mechanism leading to the sudden cessation of katabatic flow near the Antarctic coast by producing an upslope pressure-gradient force (Gallée and Schayes, 1992; Gallée and Pettré, 1998; Renfrew, 2004, hereafter R04). The isentropes are approximately parallel to the slope, indicating that air parcels descend adiabatically down the slope. An examination of the surface heat budget indicates that the downward sensible heat flux is in good balance with the radiative cooling of the slope (not shown). The adiabatic descent leads to the

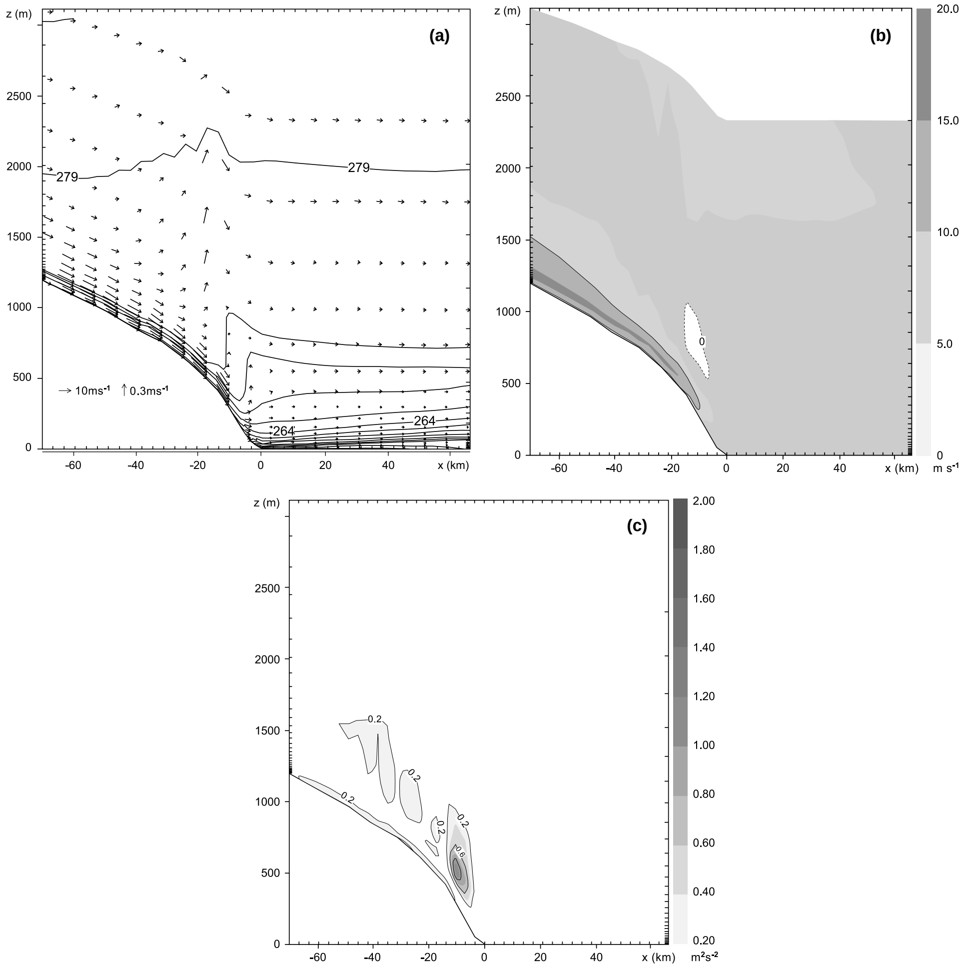

Figure 3. Model results from the control run: cross-sections of (a) θ, (b) u and (c) TKE for Grid 1. The contour intervals are 3 K, $5\,\mathrm{m\,s^{-1}}$ and $0.2\,\mathrm{m^2\,s^{-2}}$ respectively. Overplotted on (a) is the wind vector. Vectors are plotted very other grid point in horizontal and vertical directions. Scaling vectors are shown in the bottom left corner.

formation of a less stably stratified layer above the katabatic inversion. It should be mentioned that the unstable layer just above the katabatic layer has been observed during the Interaction Atmosphère-Glace-Océan (IAGO) field experiment in Adélie Land, Antarctica (PA91) and has been thought to be important for the formation of the katabatic jump. In contrast to the katabatic flow near the surface of the slope, an upslope flow (the white area enclosed by a dashed curve in Figure 3b) appears above the katabatic layer in the less stably stratified layer near the foot of the slope, suggesting the strong influence of the reverse pressure-gradient force associated with the horizontal

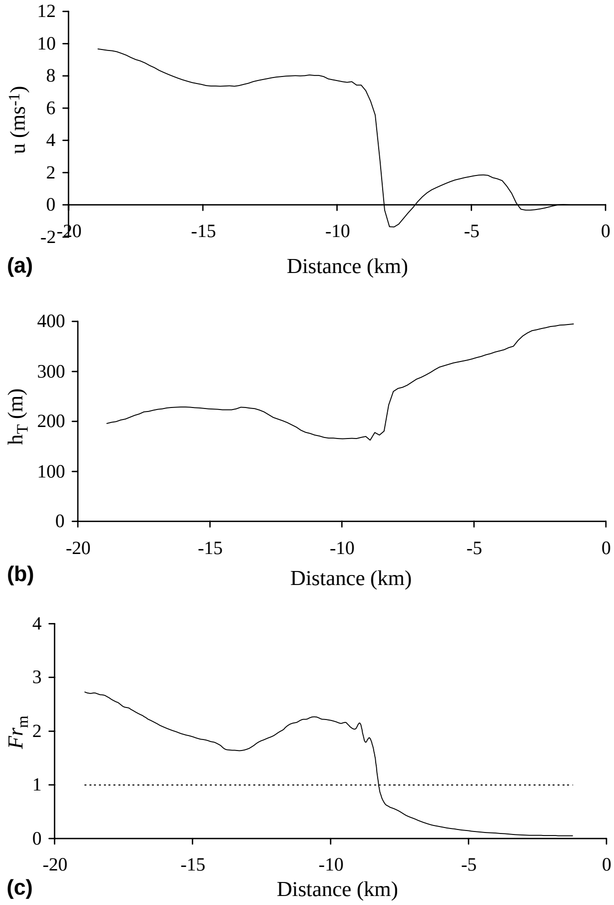

Figure 4. The simulated results at the first model level (about 2.5 m above the surface) for Grid 3 of the control run: (a) downslope component of wind (u), (b) the depth of katabatic layer (h_T), (c) the mean Froude number (Fr_m).

temperature gradient resulting from the adiabatic warming of the upper downslope airflow. Relatively high turbulent kinetic energy is produced in the near neutral or unstable area, and a less intensive turbulent region associated with the strong wind shear near the top of the katabatic layer is also obvious in Figure 3c. The role of turbulent mixing near the top of the katabatic layer in the development of katabatic jumps will be presented in a later paper.

To examine the flow characteristics simulated in the control run, the Froude number from the model fields was computed. The mean Froude number (Fr_m) is defined as follows, following Heinemann (1999, 2002),

$$Fr_m = \frac{\theta_0 u_m^2}{g h_T \, \Delta\theta}. \tag{1}$$

For the model simulations, h_T is defined as the height from the ground to the point in the θ versus z profile where the increase of potential temperature with height falls below $0.01\,\mathrm{K\,m^{-1}}$ (this is a typical potential temperature gradient in the free atmosphere above the Brunt Ice Shelf, King, 1993). Values between 0.01 and $0.05\,\mathrm{K\,m^{-1}}$ were also tested and results indicate that the flow depth is insensitive to the threshold value of stratification. In particular the abrupt change of Froude number from supercritical to subcritical is not affected by the selection of the threshold value. A similar approach was also employed by R04. In Equation (1), θ_0 is the potential temperature at h_T, u_m is the mean wind speed in the layer below h_T, $\Delta\theta$ is the potential temperature deficit (difference between the averaged potential temperature below h_T and θ_0), and g is the acceleration due to gravity. This definition of Froude number forces a two-layer structure on a continuously stratified fluid, but it is a good approximation and is appropriate for our analysis (see the results of Grid 3 in Figure 4). The calculated Froude number based on Equation (1) for Grid 3 is depicted in Figure 4c, together with the downslope wind component (u) at the first model level (Figure 4a) and katabatic layer depth h_T (Figure 4b). It can be seen that the sudden decrease of u around -8 km is accompanied by a change of the mean Froude number from supercritical ($Fr_m > 1$) to subcritical ($Fr_m < 1$) and an increase in the cold katabatic layer depth, both of which are characteristics of hydraulic jumps in open channel flows, suggesting that a katabatic jump is simulated in the control run. The change of the mean Froude number upstream of the jump closely relates to the changes of the katabatic layer depth and downslope wind speed. It is noted that reversed flow is simulated downstream of the jump near the surface, suggesting that a convergence or an updraft develops through the jump. Wind reversal downstream of a katabatic jump was also observed during the IAGO experiment (PA91).

3.2. Sensitivity experiments

Experiments in open channel flows have demonstrated that both the approach Froude number and the downstream fluid depth affect the behaviour of a hydraulic jump (Henderson, 1966). The larger the upstream Froude number the stronger the hydraulic jump, while the shallower the downstream fluid depth the further downslope the jump forms. In this section, two series of sensitivity experiments are described in which the strength of the upstream low-level jet (LLJ) and the depth of the downstream inversion layer (H) were varied. All results shown in this section are from Grid 3.

3.2.1. *Sensitivity to the Upstream Low-Level Jet*

In hydraulics, the inflow Froude number is generally related to the volume flux per unit width (Q) by $Fr = Q^2/gh^3$ (where h is the inflow depth, defined here as the depth of the inversion layer h_T) and has been used to describe the flow conditions in open channels. Here the sensitivity of the simulated jump to the strength of the upstream low-level jet is investigated based on this concept. Four experiments were conducted. They differ from the control run (where $Q = Q_0$) in that the wind profile of the u component at the upstream boundary of Grid 1 used to initialize these experiments was halved (Q05), multiplied by 1.5 (Q1.5) or doubled (Q2) (see Figure 5a). These modifications were applied only to the leftmost four grid points of the upstream lateral boundary of Grid 1 and only on the u component. It is envisaged that such modifications to the upstream profiles are the result of some specific external conditions over the whole Coats Land region that are not of interest to this study. One may notice that the profile of the u component from the control run seems to be reasonable as compared to the limited wind observations available (e.g., R04). For experiment Q0, the LLJ is set to zero, i.e., a $5\,\mathrm{m\,s^{-1}}$ vertically constant wind was prescribed as the initial condition on the leftmost four grid points of the upstream lateral boundary (Figure 5a, square marks) and kept constant with time at this boundary.

The model adjusts to a new quasi-equilibrium state within 2 hrs. Results obtained after a 12-hr integration are presented in Figure 6, in which the strength of the katabatic jump is plotted as a function of the mean upstream Froude number (Fr_m) (calculated from Equation (1)). The strength of the

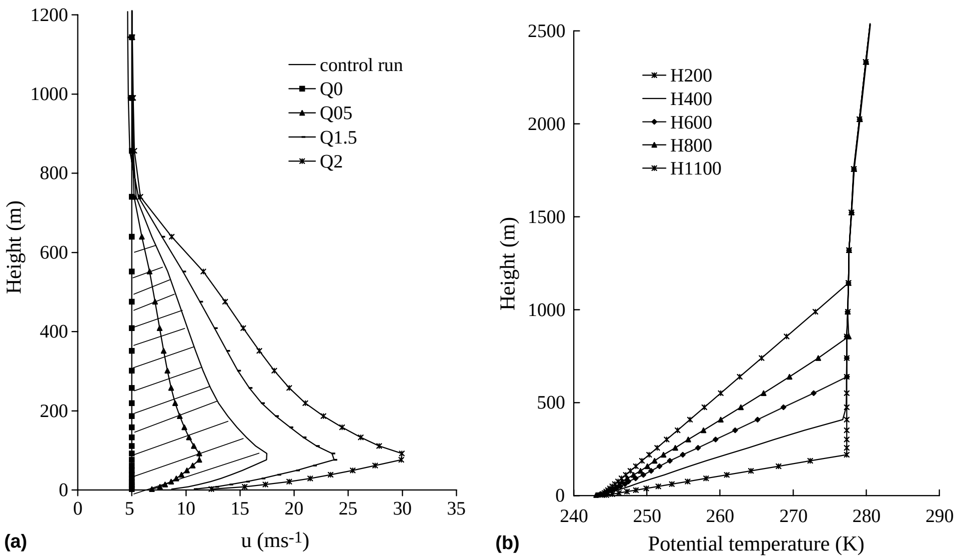

Figure 5. (a) Wind profiles (at the upstream lateral boundary of Grid 1) used to initialize experiments Q0, Q05, Q1.5, Q2 and the control run. Shaded area indicates Q in the control run, i.e., Q_0; (b) potential temperature profiles for downstream part of Grid 1 used to initialize experiments H400, H600, H800 and H1100.

katabatic jump is measured (a) as the ratio of the inversion layer depth, after (h_{T2}) and before (h_{T1}) the katabatic jump in Figure 6a, and (b) as the difference of the first model level downslope wind speed, before (u_1) and after (u_2) the jump (non-dimensionalized by the background wind u_0) in Figure 6b. The results suggest that the strength of the katabatic jump is strongly correlated to the magnitude of the upstream Froude number. As Q increases, the upstream Froude number becomes larger, and the katabatic jump becomes stronger. This parametric dependence of the katabatic jump strength on upstream mean Froude number is also common to hydraulic jumps in open channel flows, in which the strength of the hydraulic jump increases with the approach Froude number (e.g., Kawagoshi and Hager, 1990). The scale used for the katabatic jump strength in Figure 6a is similar to that used for tra-

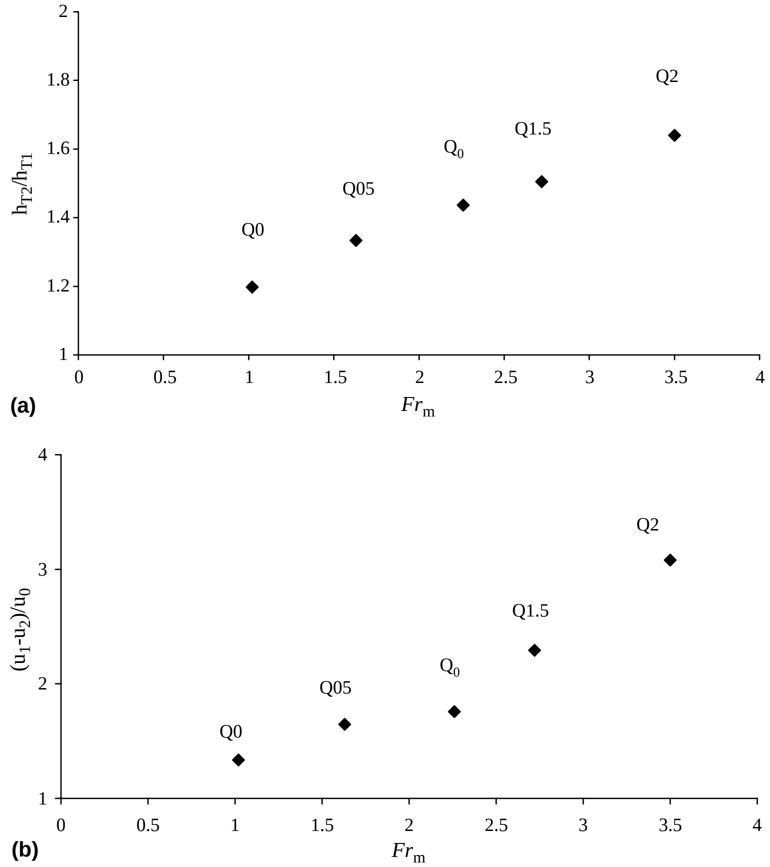

Figure 6. Two measures of the strength of a katabatic jump (see text for details) as a function of the upstream mean Froude number. Each diamond is from a different model experiment, where the upstream volume flux (Q) is varied.

ditional hydraulic jumps, while that used in Figure 6b is more suitable for meteorological applications. Both scales yield a similar trend.

A sudden rise of surface pressure across katabatic jumps has been reported by early Antarctica explorers (Lied, 1964; PA91). Here the surface pressure change (corrected to sea surface pressure) across the jumps simulated in this series of experiments (i.e., Q0, etc.) is compared to theoretical estimations. Two theories are used. The first one is a simple theory derived from the analogy to hydraulic jumps in open channel flows by Ball (1956) for describing the katabatic wind behaviour in the neighbourhood of Commonwealth Bay, Antarctica. In this theory, katabatic winds are regarded as a thin layer of cold air capped by a sharp inversion. The pressure change across the jump (Δp) is written as

$$\Delta p = \frac{\rho U_1^2}{2}\left(\frac{(1 + 8\,Fr_1)^{1/2} - 3}{Fr_1}\right), \tag{2}$$

in which ρ is the density of the cold katabatic layer and U_1 and Fr_1 are the velocity and Froude number of the upstream katabatic layer, respectively (e.g., King and Turner, 1997). Here the mean velocity (u_m) and Froude number (Fr_m) upstream of the jump defined in Section 3.1 are used as U_1 and Fr_1 respectively. Note that the Froude number used herein is different from that used in Pettré and André (1991), which is the square root of the Froude number used here. The second theory is the Boussinesq form of Bernoulli's theorem, which has been applied to katabatic jumps in Adélie Land, Antarctica and shown to give a better interpretation of the pressure changes across katabatic jumps than the simple hydraulic theory (PA91). In this approach, Bernoulli's theorem is applied to two neighbouring streamlines overlying the top of the katabatic layer and the pressure change across a katabatic jump is expressed as (after PA91):

$$\Delta p = \frac{1}{2}\rho_0(u_1^2 - u_2^2) + \rho_0 g \frac{\Delta\theta}{\hat{\theta}}\Delta z, \tag{3}$$

in which ρ_0 and $\hat{\theta}$ are the reference density and temperature, Δz is the depth of the unstable layer overlying the cold katabatic layer, and u_1 and u_2 are the downslope wind velocities on the lower and upper streamlines respectively bounding the unstable layer upstream of the jump. This equation indicates that the pressure change across a jump scales with both the wind shear due to the acceleration of the katabatic layer and the depth of the overlying unstable layer. For the modelling results, the value of u at the top of the katabatic layer, and above the unstable layer upstream of the jump, is used respectively as u_1 and u_2. The unstable layer depth (Δz) is determined as the depth of the layer with $\frac{\partial\theta}{\partial z} \leq 0$ just above the katabatic layer using the θ versus z profile immediately upstream of the jump. The reference density (ρ_0) and temperature ($\hat{\theta}$) are taken as $1.2\,\mathrm{kg\,m^{-3}}$ and 280 K, respectively. The values of u_1 and u_2, and U_1, Fr_1, $\Delta\theta$ and Δz, determined from model simulations as described in Section 3.1 and above are tabulated in Table IV.

Figure 7 shows the modelled surface pressure changes across katabatic jumps in Experiments Q0, Q05, Q1.5, Q2 and Q_0 (the control run). The pressure changes estimated from the aforementioned two theories are also shown in this figure. The general trend of the modelled pressure change across katabatic jumps with increasing Froude number is captured by both of the theories. It can be seen that the pressure changes estimated by the simple hydraulic theory (Ball, 1956; Equation (2)) are significantly smaller than those modelled by RAMS and on average only explains about 44% of the total pressure change across the katabatic jump. The deficiency of the hydraulic theory in interpreting the observed pressure change across katabatic jumps has been noted by PA91. For the two cases recorded during their IAGO experiment, PA91 found that the hydraulic theory could only account for about 30% of the observed pressure change. It should be noted that austral summer conditions prevailed during the IAGO experiment, and thus the diurnal weakening of the katabatic wind exerted an additional upslope force aiding the sudden cessation of the katabatic winds that was observed. In contrast austral winter conditions are assumed in our simulations and the sudden cessation simulated here is caused solely by cold-air damming, which probably explains the higher fraction of the pressure change that is explained by the simple hydraulic theory. The magnitudes of Δp estimated by Bernoulli's theorem (Equation (3)) are in good agreement with those modelled in RAMS for lower Froude numbers (e.g., Q05 and Q_0) and fairly good

TABLE IV

Parameters determined from model output that are used for the calculation of the pressure change across katabatic jumps in Equations (2) and (3).

Model output	Control	Q0	Q05	Q1.5	Q2
U_1 (m s^{-1})	9.7	7.26	8.58	11.8	13.7
Fr_1	2.14	1.02	1.63	2.72	3.5
u_1 (m s^{-1})	4.67	1.41	3.65	5.44	9.63
u_2 (m s^{-1})	0.05	−0.73	−1.1	−0.65	1.52
$\Delta\theta$ (K)	6.5	7	6.6	6.5	6.4
Δz (m)	185	73	133	391	450

U_1 and Fr_1 are taken as the mean velocity and Froude number of the katabatic layer upstream of the katabatic jump; u_1 and u_2 are downslope wind velocities on the lower and upper streamlines bounding the unstable layer upstream of the katabatic jump; $\Delta\theta$ is the potential temperature deficit; Δz is the depth of the unstable layer overlying the katabatic layer immediately upstream of the jump.

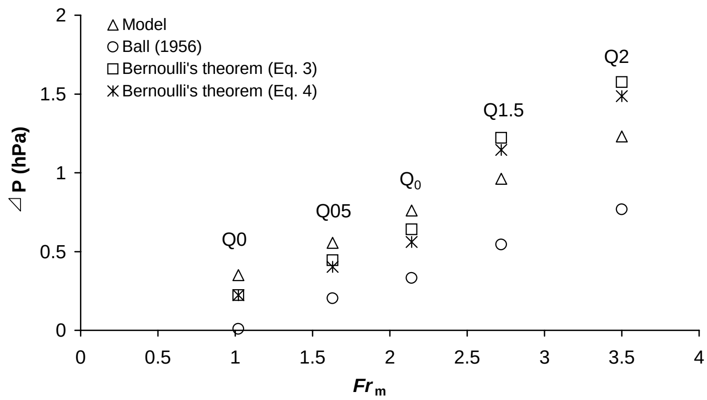

Figure 7. Surface pressure change across katabatic jump deduced from the model output and estimated from Ball's theory (1956) and Bernoulli's theorem (Equations (3) and (4)).

agreement is found for those with larger Froude numbers (e.g., Q1.5 and Q2). Applying Bernoulli's theorem to the two cases recorded in their field program, PA91 proved the success of this theorem in explaining the observed pressure change. They concluded that the pressure change was mainly linked to the strong acceleration of the downslope katabatic layer, rather than to the change in depth of the cold air layer as suggested by hydraulic theory. The results shown in Figure 7 are consistent with these conclusions. In order to compare the present results with those of PA91, the relative importance of the two terms in Equation (3) is evaluated by calculating the two terms separately for the modelled results. The results indicate that, on average, the second term on the right-hand side (i.e., the term scaled by the depth of the overlying unstable layer) explains about 67% of the modelled total pressure change across the katabatic jump, suggesting the importance of the overlying unstable layer in the development of the surface pressure change across the jump simulated in RAMS. The contribution from the second term to the total modelled pressure change is larger when compared to that indicated in PA91, which gives values of about 12% and 36% for their two cases. This discrepancy is possibly due to the uncertainties involved in the determination of $\Delta\theta$ based on the two-layer framework as mentioned in Section 3.1. Noting the large differences in the two cases in PA91 (12% and 36%), we may conclude that the overall performance of RAMS is at an acceptable level.

A few words are appropriate here about Bernoulli's theorem used by PA91. In their application the turbulent dissipation on the streamlines bounding the unstable layer was assumed to be negligible. Recently, a Bernoulli equation suitable for turbulent flow has been derived by Vosper et al. (2002), which contains a contribution from the divergence of the turbulent momentum flux. When applying this equation to the near-surface flow over a hill, it was found that the term associated with the turbulent stress is of the same order as those associated with the pressure and wind speed. Here the role of turbulent dissipation in the estimated surface pressure change across katabatic jumps is evaluated by including the turbulent stress in the Bernoulli's theorem used by PA91. Following the same procedure as deriving Equation (3) (cf. PA91), the surface pressure change across a katabatic jump, taking into account the effect of turbulent dissipation, can be written as:

$$\Delta p = \frac{1}{2}\rho_0(u_1^2 - u_2^2) + \rho_0 g \frac{\Delta\theta}{\hat{\theta}}\Delta z + \rho_0(E_1 - E_2), \qquad (4)$$

where

$$E_i = \int_{r_0}^{r_i} \left(\frac{\partial \overline{u'^2}}{\partial x} + \frac{\partial \overline{u'w'}}{\partial z} \right) dx \quad (i = 1, 2)$$

is the integral, along the lower streamline ($i = 1$) that follows the top of the katabatic layer, and the upper streamline ($i = 2$) that lies just above the overlying unstable layer, of the turbulent momentum flux divergence. The two streamlines are assumed to be very close far upstream of the jump. Other variables have the same meaning as in Equation (3). The only difference of Equation (4) from Equation (3) is the third term on the right-hand side, which is associated with the turbulent stresses on the two streamlines. The magnitude of the third term on the right-hand side of Equation (4) is estimated from model Experiments Q0, Q05, Q_0, Q1.5 and Q2 and the corresponding surface pressure changes across katabatic jumps are presented in Figure 7 (as stars). It is clear that accounting for turbulent dissipation within Bernoulli's theorem leads to a closer match between the theoretical pressure change across the jump and that modelled in RAMS, especially for strong jumps. The contribution is small (about 10%) but is an indication that turbulent momentum fluxes play a part in the dynamics of katabatic flow jumps.

3.2.2. *Sensitivity to the Downstream Inversion-Layer Depth (H)*

The retreat of hydraulic jumps with increasing downstream fluid depth has been a general fact in sloping open channel flows (Henderson, 1966). Here the impact of the downstream control mechanism is investigated using high-resolution simulations in this context. Five experiments with downstream inversion-layer depths of 219 m (H200), 409 m (H400), 640 m (H600), 856 m (H800) and 1143 m (H1100) were performed, for which only the potential temperature field was modified, i.e., other fields (u, v) were kept the same as those at the end of the 24-hr pre-integration. Figure 5b shows the vertical profiles of potential temperature used to initialize experiments H200, H400, H600, H800 and H1100, produced by linearly interpolating the potential temperature between H and the surface. These modifications were applied exclusively to the downstream part ($x > 0$) of the domain for Grid 1, and are equivalent to placing a cold-air pool in the area at the initial time. The introduced dynamical imbalance is adjusted during simulations, at time scales set by advection and wave propagation. At the end of the 12-hr integration, the flow approaches another quasi-equilibrium state. An additional experiment with zero downstream inversion-layer depth (H0) was performed and was used for momentum analysis in Section 3.3. This experiment was initialized with a neutral potential temperature profile that was applied to the downstream part of the domain for Grid 1.

The response of the jump location to the downstream inversion-layer depth is presented in Figure 8. It is seen that the depth of the downstream inversion layer has a significant influence on the location of the simulated jump, which is situated further up the slope for a deeper downstream inversion layer. The mean Froude number calculated from Equation (1) (Figure 8b) clearly shows the retreat of the supercritical flow with the increasing H (from 219 to 1143 m). Retreat of katabatic flows caused by the accumulation of cold air on the ice shelves is also simulated by R04 and is associated with an upslope pressure-gradient force produced by gradients in the potential temperature deficit and inversion height. From Figure 8b, it is noted that the strength of the jumps ($\frac{u_1-u_2}{u_0}$) slightly increases as the downstream inversion layer deepens. This is consistent with the predictions of Ball (1956)'s theory, which indicates that 'for given values of upstream flow depth and Froude number a jump moving upstream is stronger than a stationary one'. This response of the katabatic jump location to the downstream inversion-layer depth is analogous to the response of a hydraulic jump to downstream water levels in open channel flows.

Ball's (1956) theory shows that the position of a jump can be predicted using the depth of the katabatic flow and the depth of the pool of cold air over the ice shelf or ice-covered sea. Based on this theory there exists a downstream inversion depth ($\hat{h}_n$) with which the jump will be situated precisely at the foot of the slope. If the inversion-layer depth (H) near the foot of the slope exceeds the height $\hat{h}_n$ then the jump will move inland. This landward movement of a katabatic jump, in response to an increase in H, is consistent with our model results. The absence of a katabatic signature over the Brunt Ice Shelf (King, 1993; Renfrew and Anderson, 2002; R04) indicates that the characteristic inversion-layer depth over the ice shelf is generally greater than $\hat{h}_n$. Following Ball (1956), $\hat{h}_n$ can be estimated by

$$\hat{h}_n = \frac{1}{2} h_n((1 + 8\,Fr_n)^{1/2} - 1), \tag{5}$$

with $Fr_n = \frac{u_n^2}{(\theta'/\hat{\theta}) g h_n}$, in which h_n is the normal depth of the katabatic layer when the cold air has ceased to accelerate (constant flow); correspondingly u_n and Fr_n are the velocity and Froude number of this constant flow, θ' is the potential temperature deficit and $\hat{\theta}$ is the reference potential temperature. Taking typical values for Coats Land, Antarctica: $h_n = 100\,\mathrm{m}$, $u_n = 7\,\mathrm{m\,s^{-1}}$

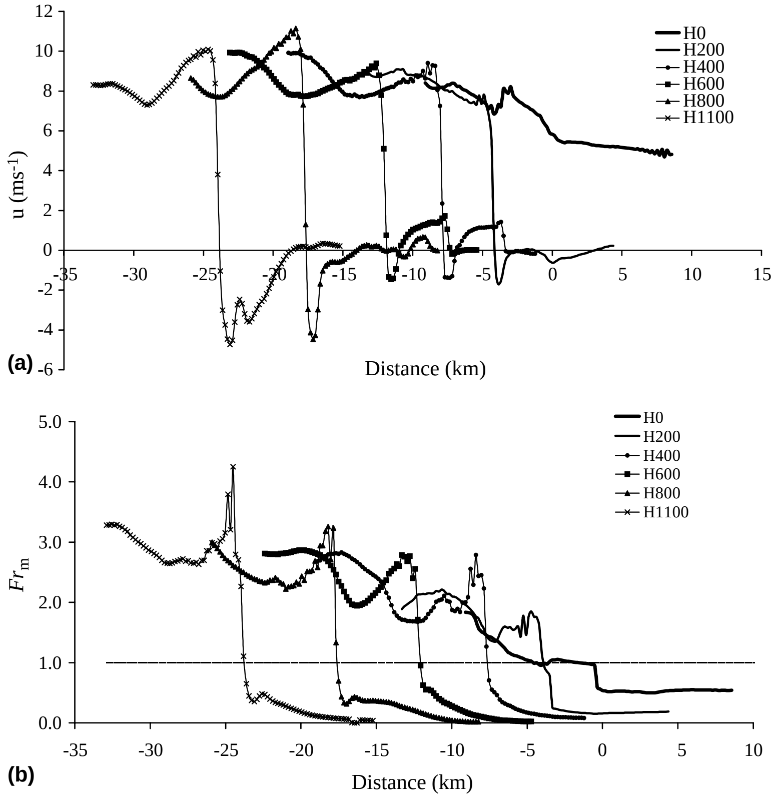

Figure 8. (a) The simulated downslope wind speed at the first model level (about 2.5 m above the surface) as a function of the distance to the foot of the slope (positive distances are on the ice shelf) for experiments H0, H200, H400, H600, H800 and H1200; and (b) mean Froude number.

and $\theta'/\hat{\theta} = 1/25$ (King, 1993; R04), we obtain $\hat{h}_n = 120\,\text{m}$ for the Coats Land area, which is obviously less than the measured inversion-layer depth of about 150 m over the ice shelf (e.g., King and Turner, 1997). The above discussion suggests that the location of the jump is basically controlled by a hydraulic response.

It should also be mentioned that the evolution of the near-surface thermal structures over the Brunt Ice Shelf has been noted by Renfrew and Anderson (2002, their Figure 7). In one of their case studies (June 1998) a cold surface layer, which is absent during a high wind period associated with a large-scale low-pressure system, is established over the ice shelf with the fading of the high winds. Consequently, the low-pressure systems that frequently travel around the Antarctic coastal regions are a possible source (mechanism) for the variation of the downstream inversion-layer depth, and in turn affect the location of any katabatic jumps. Furthermore studies on seasonal changes in the strength of the surface inversion over the Brunt Ice Shelf, based on radiosounding and infrared satellite imagery, indicate a close link between the presence of a surface inversion over the ice shelf and the existence of a 'thermal belt' on the ice slope. Such 'thermal belts' have been regarded as a sign of katabatic jumps (King et al., 1998), suggesting the existence of a favourable season or synoptic situation for the occurrence of katabatic jumps. According to King et al. (1998) the non-summer months tend to exhibit a greater number of 'thermal belt' images.

3.3. The dynamical forcing of katabatic jumps

In this section the cessation of katabatic winds in the control run is investigated by extracting the forces that make up the individual components of the momentum equation in RAMS. These forces act to accelerate or decelerate the flow and, therefore, account for its spatial variations. Previous numerical studies have suggested that the development of a katabatic jump is associated with an unstable layer overlying the katabatic layer and the cold air accumulated downstream over the ice shelves or ice-covered ocean (Gallée et al., 1996; Gallée and Pettré, 1998). In Section 3.2.1 the role of the unstable layer in the development of the surface pressure change associated with a katabatic jump was discussed. Here we focus on the role of the cold air accumulated near the foot of the slope in the formation of the katabatic jump. In fact discussions at the end of Section 3.2.2 implied the importance of the cold air near the foot of the slope.

The RAMS u-momentum equation consists of four components, i.e., pressure-gradient force (PGF); advection of momentum (ADV); momentum flux divergence force (FDIV) and Coriolis force (COR). The abbreviations in brackets are used in Figure 9. Figure 9a illustrates the forcing terms of the u-momentum budget at the first model level (about 2.5 m above the surface) extracted from RAMS at the end of the 12-hr integration for the control run. Positive values contribute to an acceleration of the katabatic flow. The dominant components are the pressure-gradient force, the advection and the momentum flux divergence. The Coriolis force is much smaller than the other components. Areas where the wind is increasing down the slope (e.g., -14 to -13 km, see Figure 4a) are marked by a positive pressure-gradient force and negative advection. Upstream of the jump, which is marked by 'J' in Figure 9a, is a phase of what Mahrt (1982) defines as 'equilibrium flow' (about -13 to -9 km), during which a positive pressure-gradient force is closely balanced by a turbulent divergence force. Near the jump, there is a reversal of the pressure-gradient force and a rapid increase in the advection force. This is accompanied, at about -8.5 km, by a sudden decrease and reversal of the katabatic flow (Figure 4a). A thorough examination of Figure 9a reveals that the jump can be divided into two phases (see the expanded scale on the

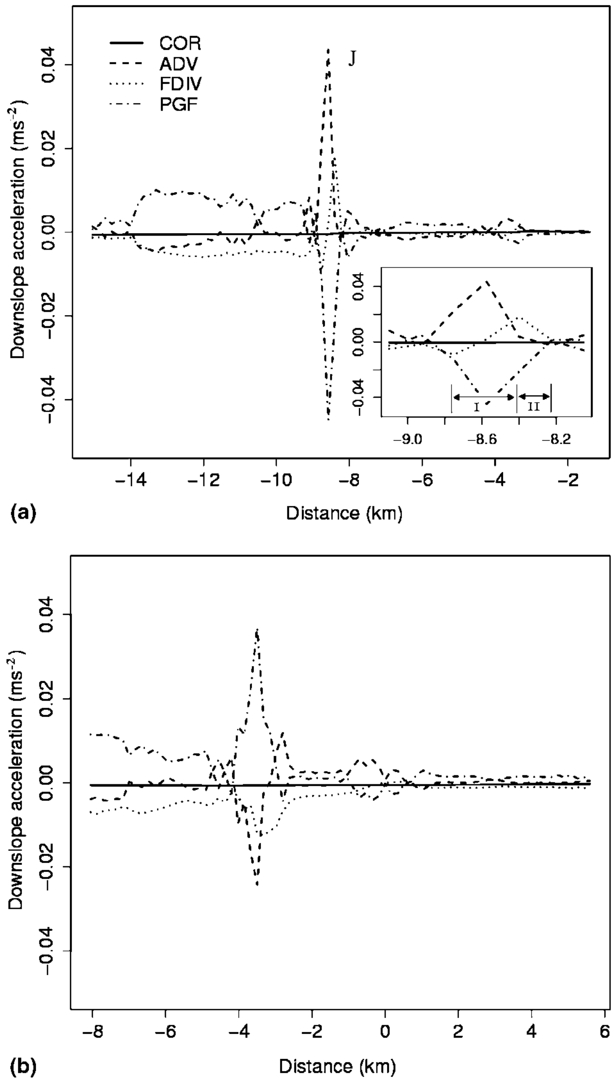

Figure 9. Downslope evolution of the forcing terms in the u-momentum equation at the end of the 12-hr simulation after the 24-hr pre-integration: (a) control run, (b) experiment H0. The details around the jump (marked by J on (a)) is shown on an expanded scale on the right bottom of (a).

bottom right of Figure 9a). In phase I the turbulent divergence force is less important and the negative pressure-gradient force is nearly balanced by the advective acceleration; in phase II (at the end of the jump), the pressure-gradient force is counterbalanced by the turbulent mixing, which mixes momentum down from the upper layer where the stronger winds still exist. Such behaviour may be correlated to the fact that the horizontal pressure contrast across the jump is stronger at the surface and the flow decelerates from the surface. After the jump, the flow changes to a phase of what Mahrt (1982) defines as 'advective-gravity flow', with positive pressure-gradient force being balanced by downslope advection of weaker momentum, explaining the recovery of the downslope wind after the jump (see Figure 4a). It is noted that before phase I there is a narrow phase where the negative pressure-gradient and turbulent flux divergence forces act simultaneously to decelerate the flow. As this phase has only one grid mesh, future studies with higher spatial resolution are needed to identify this unambiguously.

Figure 9b shows the downslope evolution of the individual components of the u-momentum equation for an extreme case (simulation H0) in which no inversion layer exists at the downstream part of the smaller domain, i.e., a neutral layer is prescribed as the initial condition. The downslope wind component at the first model level and the mean Froude number for this case are illustrated in Figures 8a and b as thick solid lines. It can be seen from Figure 8 that the jump simulated in the control run disappears in this run with katabatic winds descending vigorously onto the ice shelf. An examination of Figure 9b reveals that, after a phase of 'equilibrium flow' (between about -7 and -4 km), an 'advective-gravity flow' stage is established with the positive pressure-gradient force being nearly balanced by advection. This is also indicated in Figure 8a by an increase of the katabatic flow between -4 and -3 km. After a short 'equilibrium flow' stage, the pressure-gradient force becomes small and does not balance the turbulent divergence, leading to a deceleration of the katabatic flow (see Figure 8a, between -3 and 0 km).

The analysis of the momentum balances of the control run and run H0 suggests that the contribution of the cold air pool on the ice shelf to the pressure-gradient force is important in the formation of the jump simulated in the control run. Once a jump has formed, its strength is mainly determined by the upstream flow conditions, while its location is mainly controlled by the downstream inversion-layer depth.

It should be mentioned that katabatic jumps have been found to be associated with gravity waves (e.g., Enger and Grisogono, 1998). A comparison of the dynamic and thermodynamic fields from the control run to that from run H0 (not shown) indicates that the gravity waves are more intensive in the control run than in run H0 where no jump is produced, which suggests the possible role of gravity waves in the formation of katabatic jumps.

4. Summary and Conclusions

A non-hydrostatic numerical model, RAMS, has been used to investigate the development of katabatic jumps on the slopes of Coats Land, Antarctica. In the control run, which is homogenously initialized with a $5\,\mathrm{m\,s^{-1}}$ downslope-directed wind, a sudden cessation of the katabatic flow is produced near the foot of the idealized slope. The downslope evolution of the mean Froude number (Fr_{m}), computed based on a two-layer approximation, confirms that this transition is associated with a katabatic jump, in a hydraulic sense, i.e., the Froude number of the flow changes from $Fr_{\mathrm{m}} > 1$ to $Fr_{\mathrm{m}} < 1$. A series of sensitivity experiments is carried out to identify key factors affecting the strength and location of the jump, and to establish links with theoretical studies. The first set of sensitivity experiments, in which the upstream flow rates were changed by modifying the strength of the low-level jet, demonstrates that increases in upstream flow rate (equivalently the upstream Froude number) strengthens the katabatic jump. A similar response is common in hydraulic jumps in open channel flows.

Two theories have been used to examine the pressure change across katabatic jumps simulated in the control run and the first set of sensitivity experiments. It is found that Ball's (1956) theory based on the hydraulic jump analogy cannot explain the surface pressure change in these simulations, while the Boussinesq form of Bernoulli's theorem proposed by Pettré and André (1991) gives fairly good estimates for the pressure change. Both the acceleration of the katabatic flow and the unstable layer overlying the katabatic layer are found to be important for the surface pressure change across the jumps simulated here. Incorporating turbulent flux divergence terms into Bernoulli's theorem, following Vosper et al. (2002), improves the match of the theorem to the modelled pressure change still further.

The influence of the downstream inversion-layer depth was investigated in a second set of sensitivity experiments. Increasing the downstream inversion-layer depth results in the retreat of the jump, i.e., the jump is situated further up the slope and there is a slight increase in its strength. This is analogous to the response of a hydraulic jump to the downstream water levels in open channel flows. The possible effect of the synoptic conditions around Antarctic coast on the development and location of katabatic jumps is discussed.

An analysis of the near-surface momentum balance indicates that the important forces for the katabatic jump simulated in the control run are the pressure-gradient, advection, and to a lesser extent, turbulent divergence forces. The development of katabatic jumps can be divided into two phases. In the first phase, the pressure-gradient force is nearly balanced by advection; in the second phase, the pressure-gradient force is counterbalanced by turbulent mixing. The analysis of the momentum balance of a run (H0) in which no jump is simulated indicates that the upslope pressure gradient force associated with the pool of cold air over the ice shelf facilitates the formation of katabatic jumps. When the upslope pressure gradient is small or absent, no jump is formed. These results indicate that the frequently observed strong inversion over the Brunt Ice Shelf is responsible for the absence of katabatic signatures over it.

The results of this study highlight the promising future for the utilization of high-resolution numerical simulations in advancing our understanding and the predictability of the three-dimensional structure of katabatic jumps. These results are useful both for the study of katabatic winds over the Antarctic, and for the study of air quality in mountainous areas where hydraulic jumps have been frequently observed, even though they have not been well documented (e.g., Stull, 1988). Further investigations, using numerical models and three-dimensional observations, are needed to illustrate the evolution of the flow regimes in Coats Land, Antarctica.

Acknowledgements

Ye Yu is supported by The Overseas Research Students Award from U.K. Universities, a Science Studentship from The University of Birmingham, a Studentship from the School of Geography, Earth and Environmental Sciences, The University of Birmingham, and a CASE award from British Antarctic Survey, U.K. Many thanks are due to Craig Tremback of ATMET for advice in running RAMS.

References

Adolphs, U. and Wendler, G.: 1995, 'A Pilot-study on the Interactions between Katabatic Winds and Polynyas at the Adélie Coast, Eastern Antarctica', *Antarctic Sci.* **7**, 307–314.

Ball, F. K.: 1956, 'The Theory of Strong Katabatic Winds', *Aust. J. Phys.* **9**, 373–386.

Bromwich, D. H.: 1989, 'Satellite Analysis of Antarctic Katabatic Wind Behavior', *Bull. Amer. Meteorol. Soc.* **70**, 738–749.

Bromwich, D. H. and Kurtz, D. D.: 1984, 'Katabatic Wind Forcing of the Terra Nova Bay Polynya', *J. Geophys. Res.* **89**, 3561–3572.

Cotton, Sr. W. R., Pielke, R. A., Walko, R. L., Liston, G. E., Tremback, C. J., Jiang, H., McAnelly, R. L., Harrington, J. Y., Nicholls, M. E., Carrio, G. G., and McFadden J. P.: 2003, 'RAMS 2001: Current Status and Future Directions', *Meteorol. Atmos. Phys.* **82**, 5–29.

Enger, L. and Grisogono, B.: 1998, 'The Response of Bora-Type Flow to Sea Surface Temperature', *Quart. J. Roy. Meteorol. Soc.* **124**, 1227–1244.

Gallée, H. and Pettré, P.: 1998, 'Dynamical Constraints on Katabatic Wind Cessation in Adélie Land, Antarctica', *J. Atmos. Sci.* **55**, 1755–1770.

Gallée, H. and Schayes, G.: 1992, 'Dynamical Aspects of Katabatic Wind Evolution in the Antarctic Coastal Zone', *Boundary-Layer Meteorol.* **59**, 141–161.

Gallée, H., Pettré, P., and Schayes, G.: 1996, 'Sudden Cessation of Katabatic Winds in Adélie Land, Antarctica', *J. Appl. Meteorol.* **35**, 1129–1141.

Heinemann, G.: 1999, 'The KABEG' 97 Field Experiment: An Aircraft-Based Study of Katabatic Wind Dynamics over the Greenland Ice Sheet', *Boundary-Layer Meteorol.* **93**, 75–116.

Heinemann, G.: 2002, 'Aircraft-Based Measurements of Turbulence Structures in the Katabatic Flow over Greenland', *Boundary-Layer Meteorol.* **103**, 49–81.

Henderson, F. M.: 1966, *Open Channel Flow*, Macmillan, New York, 522 pp.

Kawagoshi, N. and Hager, W. H.: 1990, 'B-Jump in Sloping Channel, II', *J. Hydraulic Res.* **28**, 461–480.

King, J. C.: 1993, 'Control of Near-Surface Winds over an Antarctic Ice Shelf', *J. Geophys. Res.* **98**(D7), 12949–12953.

King, J. C. and Turner, J.: 1997, *Antarctic Meteorology and Climatology*, Cambridge University Press, Cambridge, 409 pp.

King, J. C., Varley, M. J., and Lachlan-cope, T. A.: 1998, 'Using Satellite Thermal Infrared Imagery to Study Boundary Layer Structure in an Antarctic Katabatic Wind Region', *Int. J. Remote Sens.* **19**, 3335–3348.

Lied, N. T.: 1964, 'Stationary Hydraulic Jumps in a Katabatic Flow near Davis, Antarctica, 1961', *Aust. Meteorol. Mag.* **47**, 40–51.

Louis, J. F.: 1979, 'A Parametric Model of Vertical Eddy Fluxes in the Atmosphere', *Boundary-Layer Meteorol.* **17**, 187–202.

Mahrer, Y. and Pielke, R. A.: 1979, 'A Numerical Study of the Airflow over Irregular Terrain', *Betr. Phys. Atmosph.* **50**, 98–113.

Mahrt, L.: 1982, 'Momentum Balance of Gravity Flow', *J. Atmos. Sci.* **39**, 2701–2711.

Mellor, G. L. and Yamada, T.: 1982, 'Development of a Turbulence Closure Model for Geophysical Fluid Problems', *Rev. Geophys. Space Phys.* **20**, 851–875.

Parish, T. R.: 1988, 'Surface Winds over the Antarctic Continent: A Review', *Rev. Geophys.* **26**, 169–180.

Parish, T. R.: 1992, 'On the Role of Antarctic Katabatic Winds in Forcing Large-Scale Tropospheric Motion', *J. Atmos. Sci.* **49**, 1374–1385.

Parish, T. R. and Bromwich, D. H.: 1987, 'The Surface Wind Field over the Antarctic Ice Sheets', *Nature* **328**, 51–54.

Parish, T. R., Bromwich, D. H., and Tzeng, R. Y.: 1994, 'One the Role of the Antarctic Continent in Forcing Large-Scale Circulation in the High Southern Latitudes', *J. Atmos. Sci.* **51**, 3566–3579.

Peel, D. A.: 1976, 'Snow Accumulation, Conductance and Temperature Inland from Halley Bay', *BAS Bull.* **43**, 1–13.

Pettré, P. and André, J. C.: 1991, 'Surface Pressure Change through Loewe's Phenomena and Katabatic Flow Jumps: Study of Two Cases in Adélie Land, Antarctic', *J. Atmos. Sci.* **48**, 557–571.

Pielke, R. A., Cotton, W. R., Walko, R. L., Tremback, C. J., Lyons, W. A., Grasso, L. D., Nicholls, M. E., Moran, M. D., Wesley, D. A., Lee, T. J., and Coprland, J. H.: 1992, 'A Comprehensive Meteorological Modeling System – RAMS', *Meteorol. Atmos. Phys.* **49**, 69–91.

Renfrew, I. A.: 2004, 'The Dynamics of Idealized Katabatic Flow over a Moderate Slope and Ice Shelf', *Quart. J. R. Meteorol. Soc.*, in press.

Renfrew, I. A. and Anderson, P. S.: 2002, 'The Surface Climatology of an Ordinary Katabatic Wind Regime in Coats Land, Antarctica', *Tellus* **54A**, 463–484.

Smagorinsky, J.: 1963, 'General Circulation Experiments with Primitive Equations: Part I: The Basic Experiment', *Mon. Wea. Rev.* **91**, 99–165.

Stull, R. B.: 1988, *An Introduction to Boundary-Layer Meteorology*, Kluwer Academic Publishers, London, 666 pp.

Vosper, S. B., Mobbs, S. D., and Gardiner, B. A.: 2002, 'Measurements of the Near-Surface Flow over a Hill', *Quart. J. Roy. Meteorol. Soc.* **128**, 2257–2280.

Walko, R. L., Band, L. E., Baron, J., Kittel, T. G. F., Lammers, R., Lee, T. J., Ojima, D., Pielke, R. A., Taylor, C., Tague, C., Tremback, C. J., and Vidale, P. J.: 2000, 'Coupled Atmosphere-Biophysics Hydrology Models for Environmental Modeling', *J. Appl. Meteorol.* **39**, 931–944.

Yu, Y.: 2004, *Numerical Simulations of Katabatic Flow Jumps in Antarctica*, PhD Thesis, The University of Birmingham, U.K., 194 pp.